Proposal for More MiniBooNE Antineutrino Data Taking

The MiniBooNE Collaboration

(Dated: February 4, 2009)

EXECUTIVE SUMMARY

The MiniBooNE experiment at Fermilab was designed to test the LSND evidence for neutrino oscillations [1]. The updated MiniBooNE oscillation result in neutrino mode [2] with 6.5E20 protons on target (POT) shows no significant excess of events at higher energies ($E_\nu > 475$ MeV), although a sizeable excess ($128.8 \pm 20.4 \pm 38.3$ events) is observed at lower energies ($E_\nu < 475$ MeV), where the first error is statistical and the second error is systematic. The lack of a significant excess at higher energies allows MiniBooNE to rule out simple $2 - \nu$ oscillations as an explanation of the LSND signal. However, the low-energy excess is presently unexplained. Additional antineutrino data and NuMI data may allow the collaboration to determine whether the excess is due, for example, to a neutrino neutral-current radiative interaction [3] or to neutrino oscillations involving sterile neutrinos [4–8] and whether the excess is related to the LSND signal.

At present, with 3.4E20 POT in antineutrino mode, MiniBooNE observes no excess ($-0.5 \pm 7.8 \pm 8.7$ events) at lower energies. These preliminary results are surprising as they imply an unexpected difference between neutrino and antineutrino properties. In order to confirm this possible difference, the MiniBooNE collaboration requests additional data taking in antineutrino mode, beyond the approved 5E20 POT, corresponding to a total of 1E21 POT. This additional running will take from one to three years, depending on the priority given to the Booster neutrino beam proton intensity, and will allow a detailed comparison between the neutrino and antineutrino data sets at both low and high energies. The low-energy comparison will be especially significant because the estimated backgrounds in the two modes are very similar, which allows a significant reduction in the systematic uncertainties when comparing neutrinos to antineutrinos. If, for example, there continues to be no low-energy excess in antineutrino mode with 1E21 POT, then the hypothesis that the excess scales as the neutrino flux (and not the antineutrino flux) would be confirmed and other hypotheses ruled out at $> 98\%$ CL.

In addition, the high energy antineutrino data will provide a direct test of the LSND signal and will increase the statistics of the NuMI data sample. With the present 3.4E20 POT in antineutrino mode, almost all of the LSND region is still allowed, as the current limit is worse than the sensitivity. However, with 1E21 POT in the case of no neutrino oscillations, most of the LSND allowed region should be ruled out. In the case of neutrino

oscillations at the LSND best-fit point, a $\sim 1.5\sigma$ event excess would be expected.

INTRODUCTION

Evidence for neutrino oscillations comes from solar-neutrino [9–13] and reactor-antineutrino experiments [14], which have observed ν_e disappearance at $\Delta m^2 \sim 8 \times 10^{-5}$ eV^2, and atmospheric-neutrino [15–18] and long-baseline accelerator-neutrino experiments [19, 20], which have observed ν_μ disappearance at $\Delta m^2 \sim 3 \times 10^{-3}$ eV^2. In addition, the LSND experiment [1] has presented evidence for $\bar{\nu}_\mu \rightarrow \bar{\nu}_e$ oscillations at the $\Delta m^2 \sim 1$ eV^2 scale. If all three phenomena are caused by neutrino oscillations, these three Δm^2 scales cannot be accommodated in an extension of the Standard Model that has only three neutrino mass eigenstates. An explanation of all three mass scales with neutrino oscillations requires the addition of one or more sterile neutrinos [4–8] or further extensions of the Standard Model (*e.g.,* [21]).

The MiniBooNE experiment was designed to test the neutrino oscillation interpretation of the LSND signal in both neutrino and antineutrino modes. MiniBooNE has approximately the same L/E_ν as LSND but with an order of magnitude higher baseline and energy. Due to the higher energy and dissimilar event signature, MiniBooNE systematic errors are completely different from LSND errors. MiniBooNE's updated oscillation results in neutrino mode [2] show no significant excess of events at higher energies; however, a sizeable excess of events is observed at lower energies, as shown in Fig. 1. Although the excess energy shape does not fit two-neutrino oscillations, the number of excess events is similar to the LSND expectation. At present, with 3.4E20 POT in antineutrino mode, MiniBooNE observes no excess at lower energies.

MINIBOONE

Neutrino Oscillation Event Selection

MiniBooNE searches for $\nu_\mu \rightarrow \nu_e$ oscillations by measuring the rate of $\nu_e C \rightarrow e^- X$ CCQE events and testing whether the measured rate is consistent with the estimated background rate. To select candidate ν_e CCQE events, an initial selection is first applied: > 200 tank hits, < 6 veto hits, reconstructed time within the neutrino beam spill, reconstructed vertex
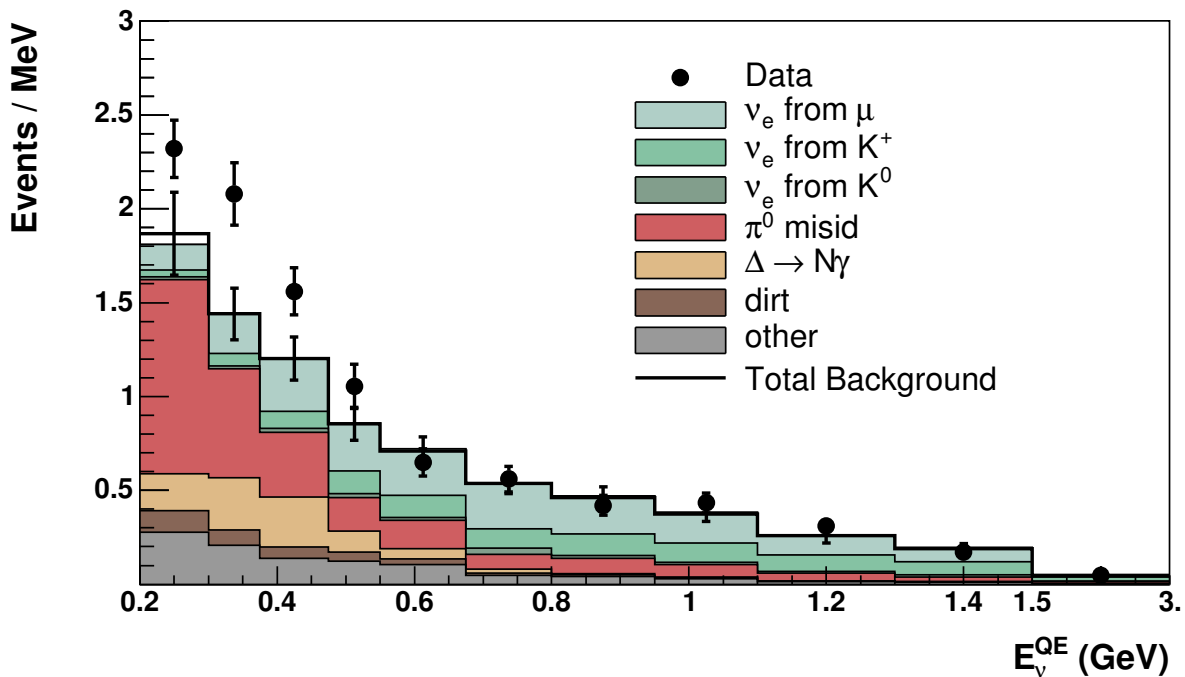
FIG. 1: *The MiniBooNE reconstructed neutrino energy distribution for candidate ν_e data events (points with error bars) compared to the Monte Carlo simulation (histogram) [2] for the neutrino data sample.*

radius < 500 cm, and visible energy $E_{vis} > 140$ MeV. It is then required that the electron-hypothesis event vertex and muon-hypothesis track endpoint occur at radii < 500 cm and < 488 cm, respectively, to ensure good event reconstruction and effective rejection of possible muon decay electrons. Particle identification (PID) cuts are then applied to reject muon and π^0 events. Several improvements have been made to the neutrino oscillation data analysis since the initial data was published [2], including an improved background estimate, an additional fiducial volume cut that greatly reduces the background from events produced outside the tank (dirt events), and an increase in the data sample from 5.579×10^{20} POT to 6.462×10^{20} POT. A total of 89,200 neutrino events pass the initial selection, while 1069 events pass the complete event selection of the Final Analysis with $E_\nu^{QE} > 200$ MeV.

Neutrino Oscillation Signal and Background Reactions

Table I shows the expected number of candidate ν_e CCQE background events with E_ν^{QE} between $200 - 300$ MeV, $300 - 475$ MeV, and $475 - 1250$ MeV after the Final Analysis event

TABLE I: *The expected number of events in the* $200 < E_\nu^{QE} < 300$ *MeV*, $300 < E_\nu^{QE} < 475$ *MeV, and* $475 < E_\nu^{QE} < 1250$ *MeV energy ranges from all of the significant backgrounds after the complete event selection of the Final Analysis for the neutrino data sample. Also shown are the expected number of ν_e CCQE signal events for neutrino oscillations at the LSND best-fit solution.*

Process	200 − 300	300 − 475	475 − 1250
ν_μ CCQE	9.0	17.4	11.7
$\nu_\mu e \to \nu_\mu e$	6.1	4.3	6.4
NC π^0	103.5	77.8	71.2
NC $\Delta \to N\gamma$	19.5	47.5	19.4
Dirt Events	11.5	12.3	11.5
Other Events	18.4	7.3	16.8
ν_e from μ Decay	13.6	44.5	153.5
ν_e from K^+ Decay	3.6	13.8	81.9
ν_e from K_L^0 Decay	1.6	3.4	13.5
Total Background	186.8 ± 26.0	228.3 ± 24.5	385.9 ± 35.7
LSND Best-Fit Solution	7 ± 1	37 ± 4	135 ± 12

selection. The background estimate includes antineutrino events, representing $< 2\%$ of the total. The total expected backgrounds for the three energy regions are 186.8 ± 26.0 events, 228.3 ± 24.5 events, and 385.9 ± 35.7 events, respectively. For $\nu_\mu \to \nu_e$ oscillations at the best-fit LSND solution of $\Delta m^2 = 1.2$ eV^2 and $\sin^2 2\theta = 0.003$, the expected number of ν_e CCQE signal events are included in the Table.

Updated Neutrino Oscillation Results

Fig. 1 shows the reconstructed neutrino energy distribution for candidate ν_e data events (points with error bars) compared to the MC simulation (histogram) [2], while Fig. 2 shows the event excess as a function of reconstructed neutrino energy. Good agreement between the data and the MC simulation is obtained for $E_\nu > 475$ MeV; however, an unexplained excess of electron-like events is observed for $E_\nu < 475$ MeV. As shown in Fig. 2, the
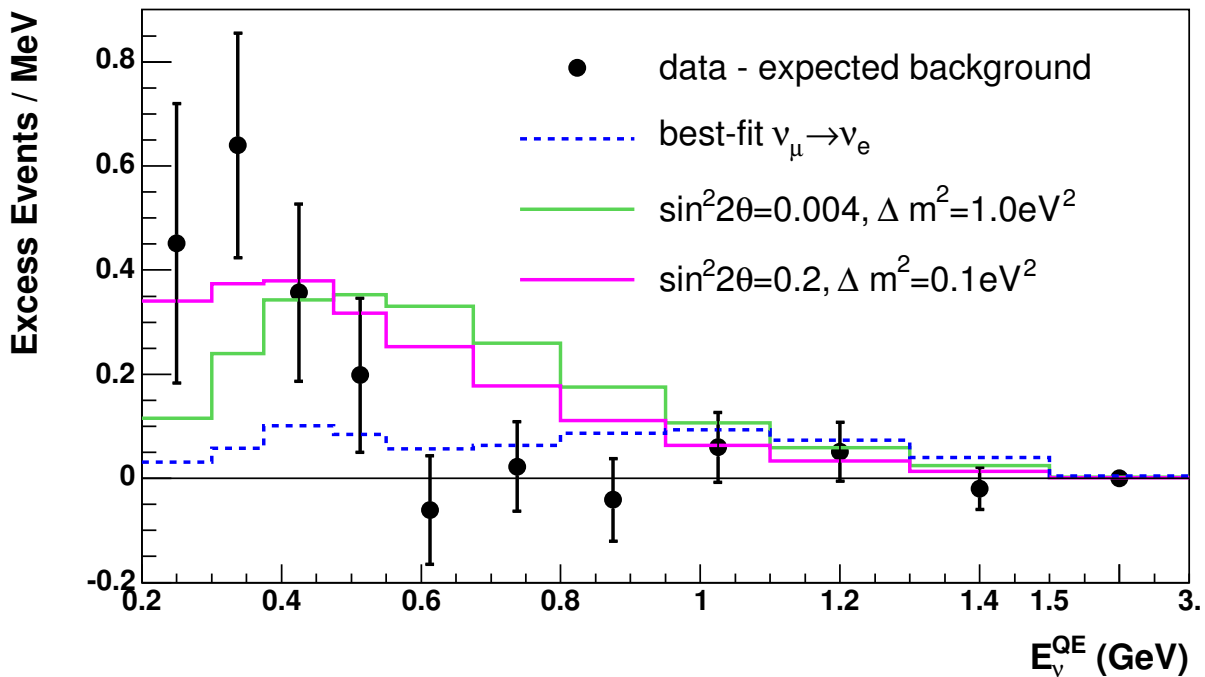
FIG. 2: *The neutrino event excess as a function of E_ν^{QE} for the neutrino data sample. Also shown are the expectations from the best oscillation fit ($\sin^2 2\theta = 0.0017$, $\Delta m^2 = 3.14\ eV^2$) and from neutrino oscillation parameters in the LSND allowed region [1]. The error bars include both statistical and systematic errors.*

magnitude of the excess is very similar to what is expected from neutrino oscillations based on the LSND signal. Although the shape of the excess is not consistent with simple two-neutrino oscillations, more complicated oscillation models [4–8] may be consistent with both the LSND and MiniBooNE signals.

Table II shows the number of data, background, and excess events for different E_ν^{QE} ranges, together with the significance of the excess. For the Final Analysis, an excess of $128.8 \pm 20.4 \pm 38.3$ events is observed for $200 < E_\nu^{QE} < 475$ MeV. For the entire $200 < E_\nu^{QE} < 1250$ MeV energy region, the excess is $151.0 \pm 28.3 \pm 50.7$ events. As shown in Fig. 3, the event excess occurs for $E_{vis} < 400$ MeV, where E_{vis} is the visible energy.

Figs. 4 and 5 show the event excess as functions of Q^2 and $\cos(\theta)$ for $300 < E_\nu^{QE} < 475$ MeV, where Q^2 is determined from the energy and angle of the outgoing lepton and θ is the angle between the beam direction and the reconstructed event direction. Also shown in the figures are the expected shapes from $\nu_e C \rightarrow e^- X$ and $\bar{\nu}_e C \rightarrow e^+ X$ charged-current (CC) scattering and from the NC π^0 and $\Delta \rightarrow N\gamma$ reactions, which are representative of photon

TABLE II: *The number of data, background, and excess events for different E_ν^{QE} ranges, together with the significance of the excesses for the neutrino data sample.*

Event Sample	Final Analysis
200 − 300 MeV	
Data	232
Background	$186.8 \pm 13.7 \pm 22.1$
Excess	$45.2 \pm 13.7 \pm 22.1$
Significance	1.7σ
300 − 475 MeV	
Data	312
Background	$228.3 \pm 15.1 \pm 19.3$
Excess	$83.7 \pm 15.1 \pm 19.3$
Significance	3.4σ
200 − 475 MeV	
Data	544
Background	$415.2 \pm 20.4 \pm 38.3$
Excess	$128.8 \pm 20.4 \pm 38.3$
Significance	3.0σ
475 − 1250 MeV	
Data	408
Background	$385.9 \pm 19.6 \pm 29.8$
Excess	$22.1 \pm 19.6 \pm 29.8$
Significance	0.6σ

events produced by NC scattering. The NC scattering assumes the ν_μ energy spectrum, while the CC scattering assumes the transmutation of ν_μ into ν_e and $\bar{\nu}_e$, respectively. As shown in Table III, the χ^2 values from comparisons of the event excess to the expected shapes are acceptable for all of the processes. However, any of the backgrounds in Table III would have to be increased by $> 5\sigma$ to explain the low-energy excess.
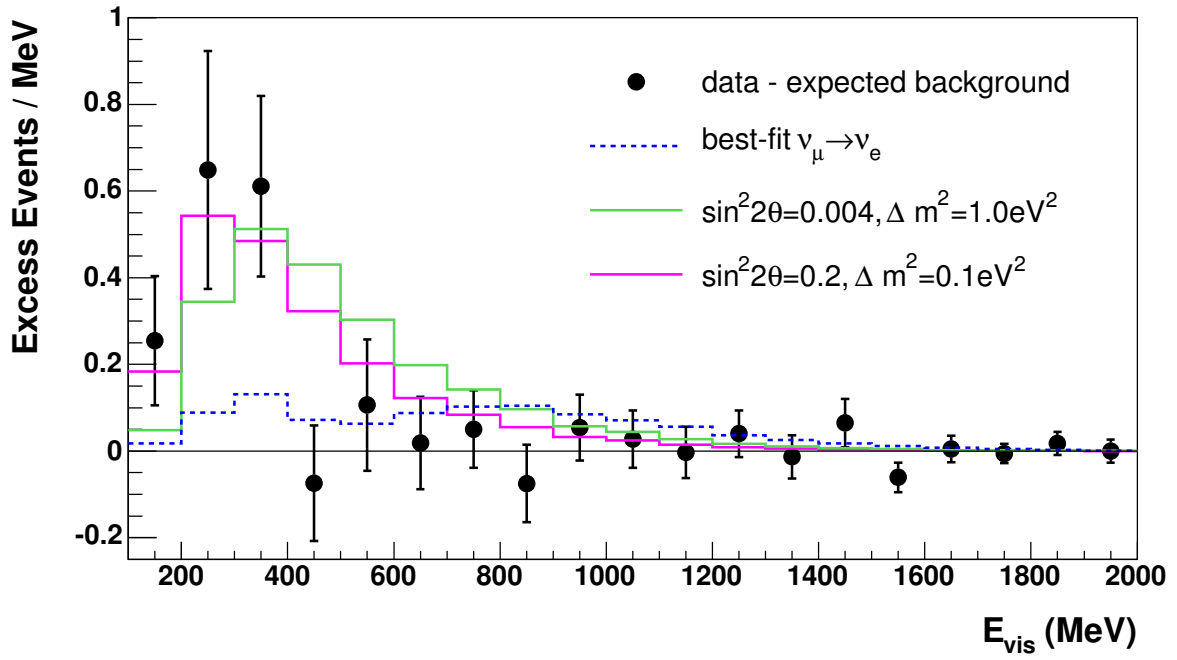
FIG. 3: *The event excess as a function of E_{vis} for $E_{\nu}^{QE} > 200\ MeV$ for the neutrino data sample. Also shown are the expectations from the best oscillation fit ($\sin^2 2\theta = 0.0017$, $\Delta m^2 = 3.14\ eV^2$) and from neutrino oscillation parameters in the LSND allowed region [1]. The error bars include both statistical and systematic errors.*
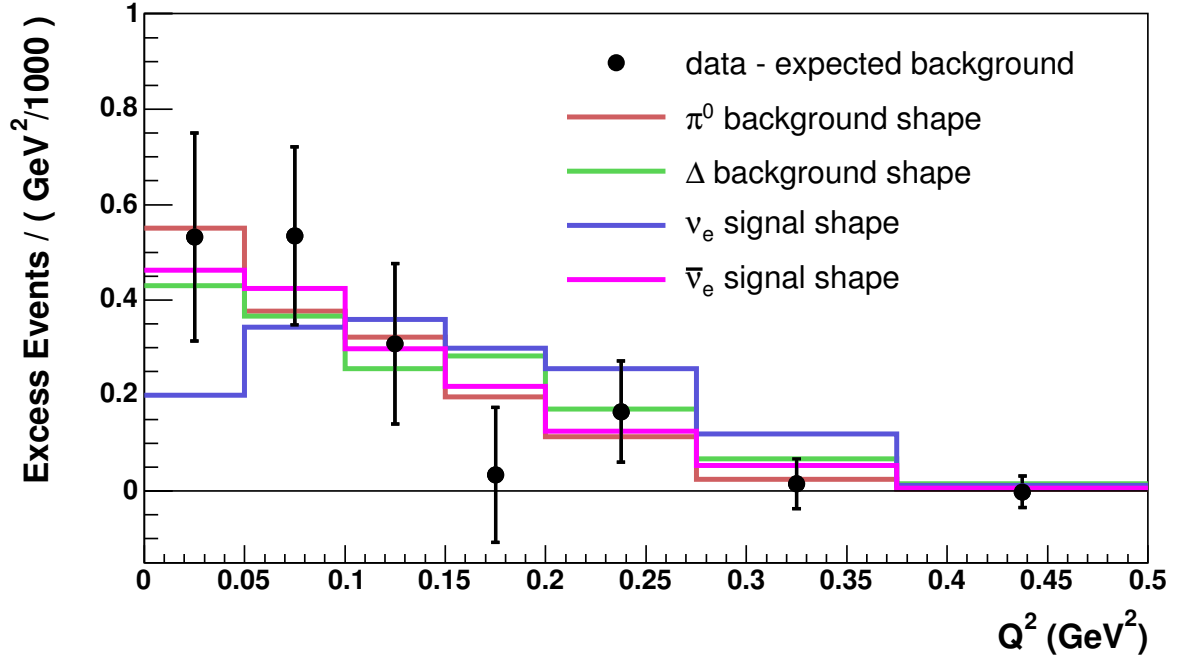

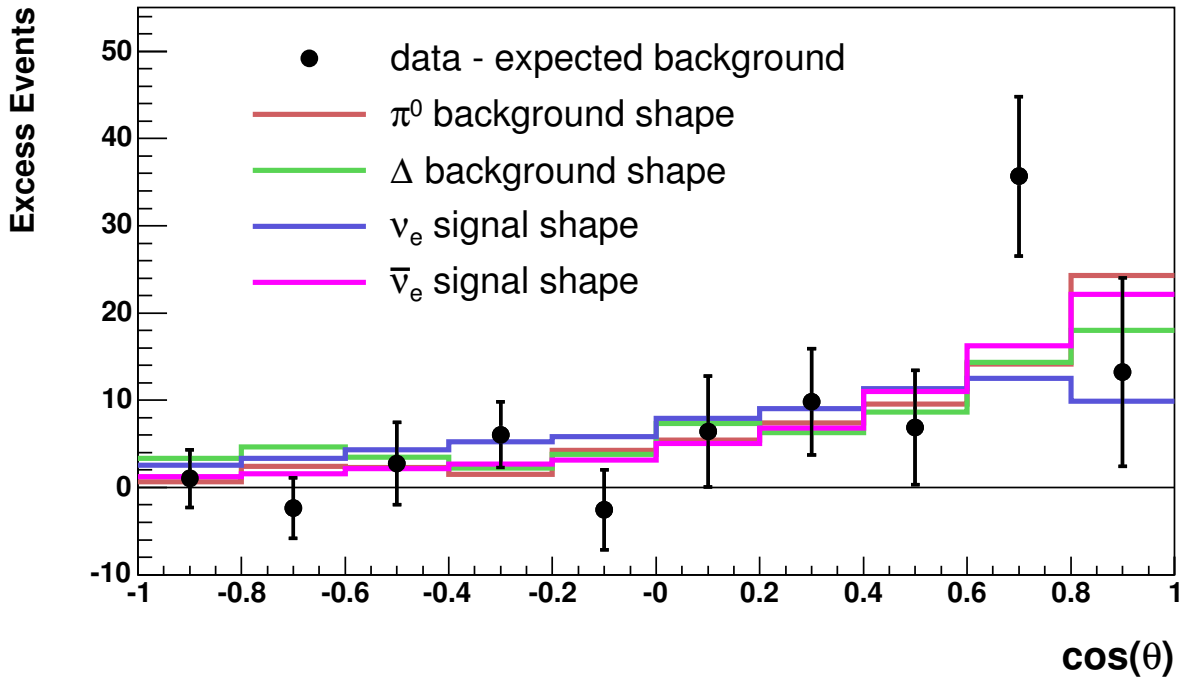FIG. 4: *The event excess as a function of Q^2 for $300 < E_{\nu}^{QE} < 475\ MeV$ for the neutrino data sample.*

FIG. 5: *The event excess as a function of* $\cos(\theta)$ *for* $300 < E_\nu^{QE} < 475$ *MeV for the neutrino data sample.*

TABLE III: *The* χ^2 *values from comparisons of the event excess* Q^2 *and* $\cos(\theta)$ *distributions for* $300 < E_\nu^{QE} < 475$ *MeV to the expected shapes from various NC and CC reactions for the neutrino data sample. Also shown is the factor increase necessary for the estimated background for each process to explain the low-energy excess.*

Process	$\chi^2(\cos\theta)$/9 DF	$\chi^2(Q^2)$/6 DF	Factor Increase
NC π^0	13.46	2.18	2.0
$\Delta \to N\gamma$	16.85	4.46	2.7
$\nu_e C \to e^- X$	14.58	8.72	2.4
$\bar{\nu}_e C \to e^+ X$	10.11	2.44	65.4

Preliminary Antineutrino Oscillation Results

The same analysis that was used for the neutrino oscillation results is employed for the antineutrino oscillation results. Fig. 6 shows the estimated neutrino fluxes for neutrino mode and antineutrino mode. The fluxes are fairly similar (the intrinsic electron-neutrino
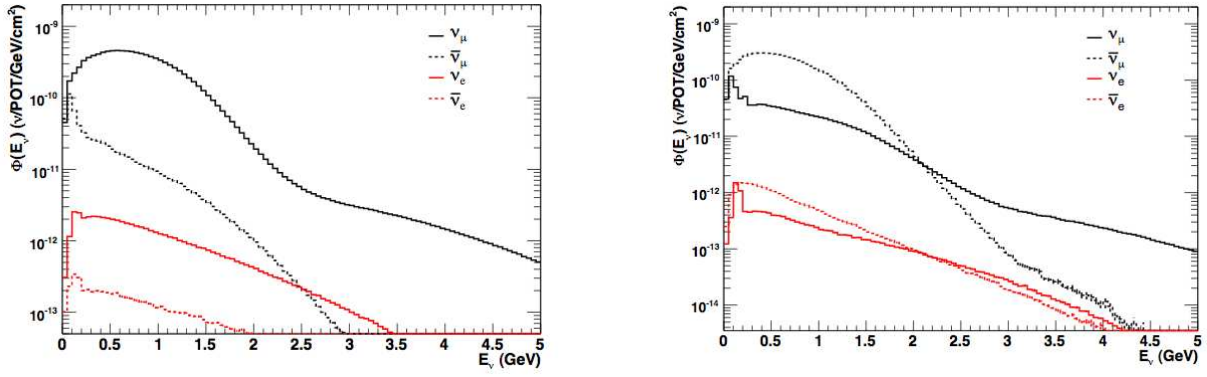
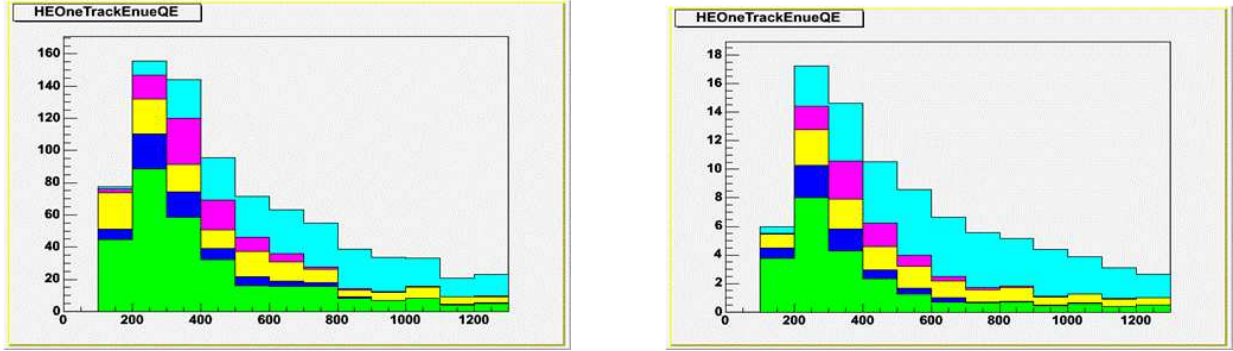FIG. 6: *The estimated neutrino fluxes for neutrino mode (left plot) and antineutrino mode (right plot).*

FIG. 7: *The estimated backgrounds for the neutrino oscillation search in neutrino mode (left plot) and antineutrino mode (right plot). The π^0, $\Delta \to N\gamma$, intrinsic $\nu_e/\bar{\nu}_e$, external event, and other backgrounds correspond to the green, pink, light blue, blue, and yellow colors, respectively.*

background is approximately 0.5% for both modes of running), although the wrong-sign contribution to the flux in antineutrino mode ($\sim 18\%$) is much larger than in neutrino mode ($\sim 6\%$). The average ν_e plus $\bar{\nu}_e$ energies are 0.96 GeV in neutrino mode and 0.77 GeV in antineutrino mode, while the average ν_μ plus $\bar{\nu}_\mu$ energies are 0.79 GeV in neutrino mode and 0.66 GeV in antineutrino mode. Also, as shown in Fig. 7, the estimated backgrounds in the two modes are very similar, especially at low energy. Fig. 8 shows the expected antineutrino oscillation sensitivity for the present data sample corresponding to 3.4E20 POT. The two sensitivity curves correspond to threshold neutrino energies of 200 MeV and 475 MeV.

The preliminary oscillation results for antineutrino mode are shown in Table IV and Figs. 9 through 11. It is quite surprising that no excess ($-0.5 \pm 7.8 \pm 8.7$ events) is observed in the low-energy range $200 < E_\nu^{QE} < 475$ MeV. In order to understand the implications that the antineutrino data have on the neutrino low-energy excess, Table V shows the
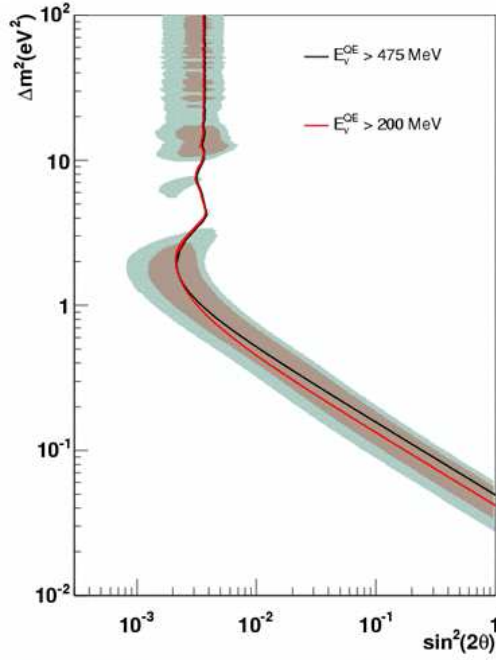
FIG. 8: *The expected antineutrino oscillation sensitivity at 90% CL for the present data sample corresponding to 3.4E20 POT. The two sensitivity curves correspond to threshold energies of 200 MeV (red curve) and 475 MeV (black curve).*

expected excess of low-energy events in antineutrino mode under various hypotheses. These hypotheses include the following:

- Same σ: Same cross section for neutrinos and antineutrinos.

- π^0 Scaled: Scaled to number of neutral-current π^0 events.

- POT Scaled: Scaled to number of POT.

- BKGD Scaled: Scaled to total background events.

- CC Scaled: Scaled to number of charged-current events.

- Kaon Scaled: Scaled to number of low-energy kaon events.

- Neutrino Scaled: Scaled to number of neutrino events.

Also shown in Table V is the probability (from a two-parameter fit to the data) that each hypothesis explains the observed number of low-energy neutrino and antineutrino events,

TABLE IV: *The number of data, background, and excess events for different E_ν^{QE} ranges, together with the significance of the excesses for the antineutrino data sample.*

Event Sample	Final Analysis
$200 - 475$ MeV	
Data	61
Background	$61.5 \pm 7.8 \pm 8.7$
Excess	$-0.5 \pm 7.8 \pm 8.7$
Significance	-0.04σ
$475 - 1250$ MeV	
Data	61
Background	$57.8 \pm 7.6 \pm 6.5$
Excess	$3.2 \pm 7.6 \pm 6.5$
Significance	0.3σ
$475 - 3000$ MeV	
Data	83
Background	$77.4 \pm 8.8 \pm 9.6$
Excess	$5.6 \pm 8.8 \pm 9.6$
Significance	0.4σ

assuming only statistical errors, correlated systematic errors, and uncorrelated systematic errors. A proper treatment of the systematic errors is in progress; however, it is clear from the Table that the "Neutrino Scaled" hypothesis fits best and that the "Same σ", "POT Scaled", and "Kaon Scaled" hypotheses are strongly disfavored. It will be very important to understand this unexpected difference between neutrino and antineutrino properties.

The antineutrino data were also fit for oscillations in the energy range $475 < E_\nu^{QE} < 3000$ MeV, assuming antineutrino oscillations but no neutrino oscillations. The antineutrino oscillation allowed region is shown in Fig. 12. At present, the oscillation limit is worse than the sensitivity. The best oscillation fit corresponds to $\Delta m^2 = 4.4$ eV^2, $\sin^2 2\theta = 0.0047$, and a fitted excess of 18.6 ± 13.2 events, which is consistent with the LSND best fit point of $\Delta m^2 = 1.2$ eV^2, $\sin^2 2\theta = 0.003$, and an expected excess of 14.7 events. With the present
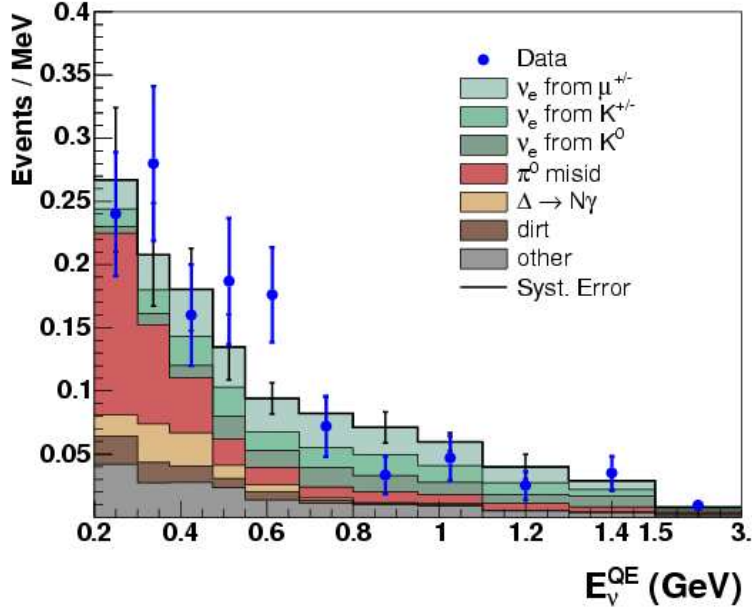
FIG. 9: *The comparison between data and Monte Carlo expectation as a function of reconstructed neutrino energy for the present antineutrino data sample corresponding to 3.4E20 POT.*

TABLE V: *The expected excess of low-energy events in antineutrino mode under various hypotheses for 3.4E20 POT. Also shown in the Table is the probability (from a two-parameter fit to the data) that each hypothesis explains the observed number of low-energy neutrino and antineutrino events, assuming only statistical errors, correlated systematic errors, and uncorrelated systematic errors.*

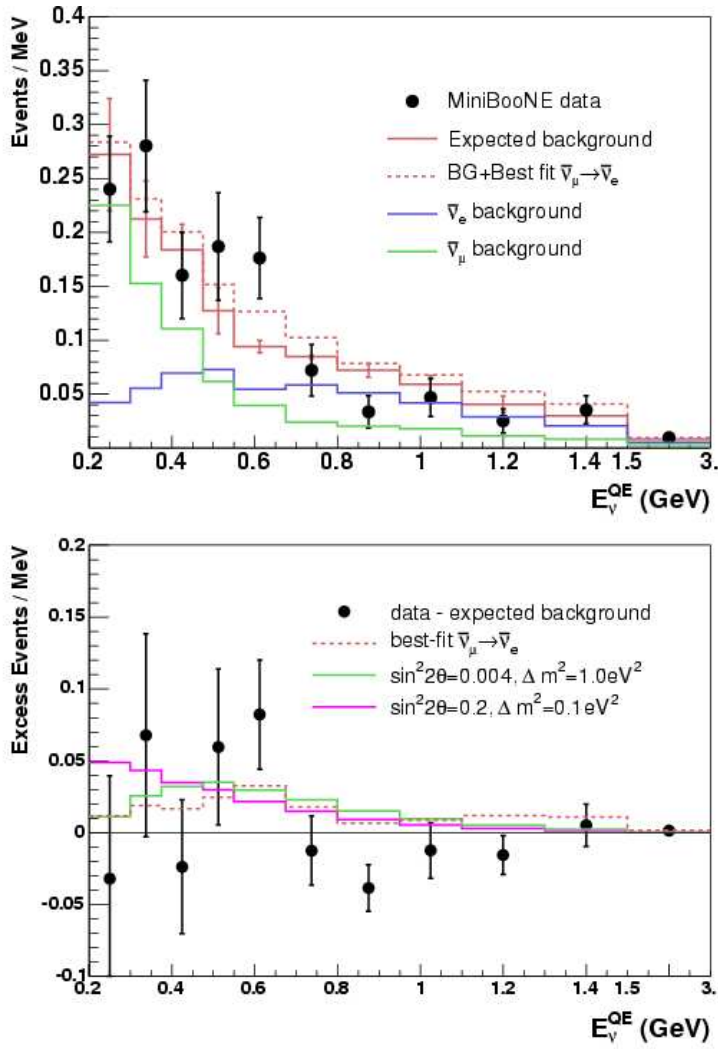| Hypothesis	Expec. # of $\bar{\nu}$ Events	Stat. Err.	Cor. Syst. Err.	Uncor. Syst. Err.
Same σ	37.2	0.1%	0.1%	6.7%
π^0 Scaled	19.4	3.6%	6.4%	21.5%
POT Scaled	67.5	0.0%	0.0%	1.8%
BKGD Scaled	20.9	2.7%	4.7%	19.2%
CC Scaled	20.4	2.9%	5.2%	19.9%
Kaon Scaled	39.7	0.1%	0.1%	5.9%
Neutrino Scaled	6.7	38.4%	51.4%	58.0%

13

FIG. 10: *The comparison between data and Monte Carlo expectation (top) and the excess number of events (bottom) as a function of reconstructed neutrino energy for the present antineutrino data sample corresponding to 3.4E20 POT. Also shown are the expectations from the best oscillation fit and from oscillation parameters in the LSND allowed region.*

antineutrino statistics, the data are consistent with both the LSND best-fit point and the null point, although the LSND best-fit point has a better χ^2 ($\chi^2 = 17.63/16$ DF, probability $= 34.6\%$) than the null point ($\chi^2 = 22.19/16$ DF, probability $= 13.7\%$).
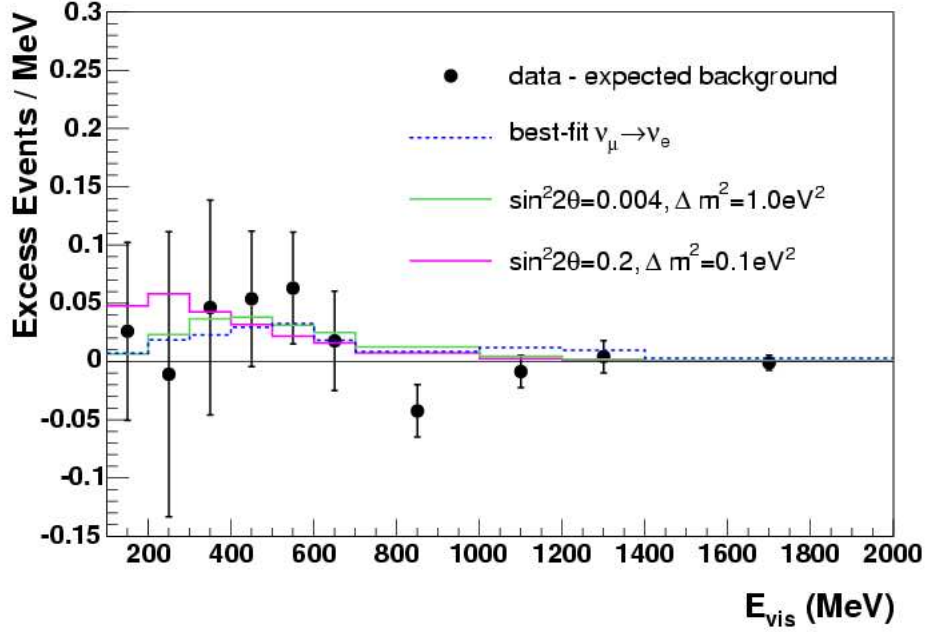
14

FIG. 11: *The excess number of events (data minus Monte Carlo expectation) as a function of visible energy for the present antineutrino data sample corresponding to 3.4E20 POT. Also shown are the expectations from the best oscillation fit and from oscillation parameters in the LSND allowed region.*

MiniBooNE NuMI Results

Neutrino events are also observed in MiniBooNE from the NuMI beam [22]. The NuMI beam, as shown in Fig. 13, differs from the Booster neutrino beam (BNB) in several respects. First, the NuMI beam is off axis by 110 mrad, whereas the BNB is on axis. Second, neutrinos from NuMI travel ~ 700 m, compared to ~ 500 m for neutrinos from the BNB. Also, the NuMI beam has a 6% contribution from electron-neutrinos and a 14% contribution from antineutrinos, while the BNB percentages are 0.5% and 2%, respectively. Fig. 14 shows the estimated neutrino flux at the MiniBooNE detector from the NuMI beam, while Fig. 15 compares the neutrino fluxes from the BNB and NuMI beams.

Figs. 16 and 17 show the comparison between data events (points with error bars) and the MC simulation (histogram) for ν_μ CCQE candidate events and ν_e CCQE candidate events,
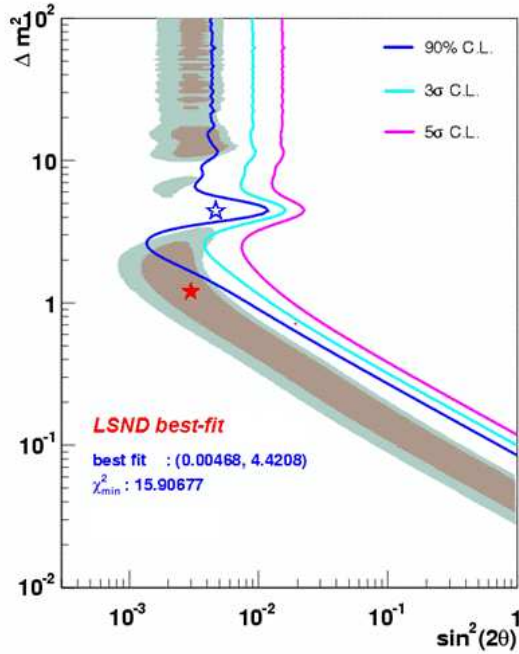
FIG. 12: *The antineutrino oscillation allowed region in the energy range $475 < E_\nu^{QE} < 3000 \ MeV$ for the present antineutrino data sample corresponding to 3.4E20 POT. Also shown are the best oscillation fit ($\Delta m^2 = 4.4 \ eV^2$, $\sin^2 2\theta = 0.0047$, and an excess of 18.6 ± 13.2 events) and the LSND best fit point ($\Delta m^2 = 1.2 \ eV^2$, $\sin^2 2\theta = 0.003$, and an excess of 14.7 events).*

respectively. Although the systematic errors are presently large, the data are observed to be systematically low for ν_μ CCQE candidate events and systematically high for ν_e CCQE candidate events. Updated results should be available soon with three times the data sample and with reduced systematic errors by constraining the normalization to the ν_μ sample.

The NuMI data analysis is currently directed toward examining the low-energy region and searching for neutrino oscillations. This will complement the analysis done with MiniBooNE using neutrino and anti-neutrino BNB data, but with different systematic errors. It is worth noting that the NuMI ν_e CCQE sample has a very different composition when compared to the BNB neutrino ν_e CCQE sample. The BNB ν_e sample originates mostly from decays of pions produced in the target and contains a large fraction of ν_μ mis-identified events. On other hand, the NuMI ν_e CCQE sample is produced mostly from the decay of kaons and contains a dominant fraction of intrinsic ν_e events. The analysis will be done by forming a correlation between the ν_μ CCQE and ν_e CCQE samples and by tuning the prediction to the data simultaneously. The result is that common systematics cancel, and this might
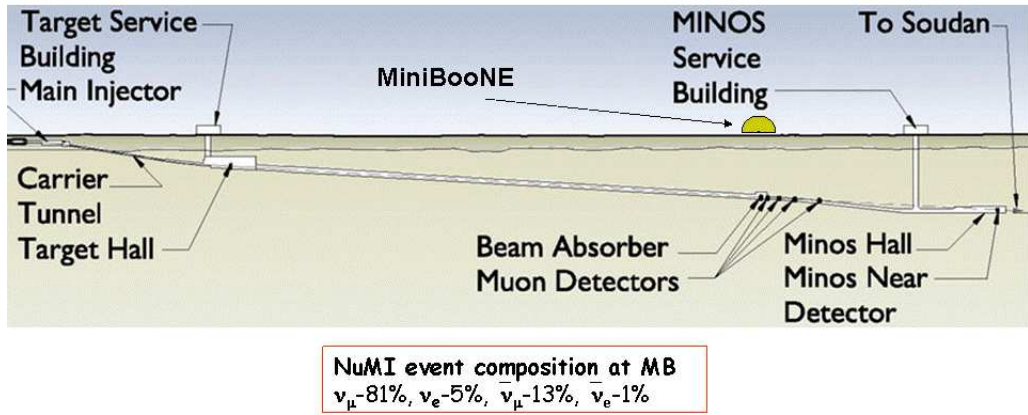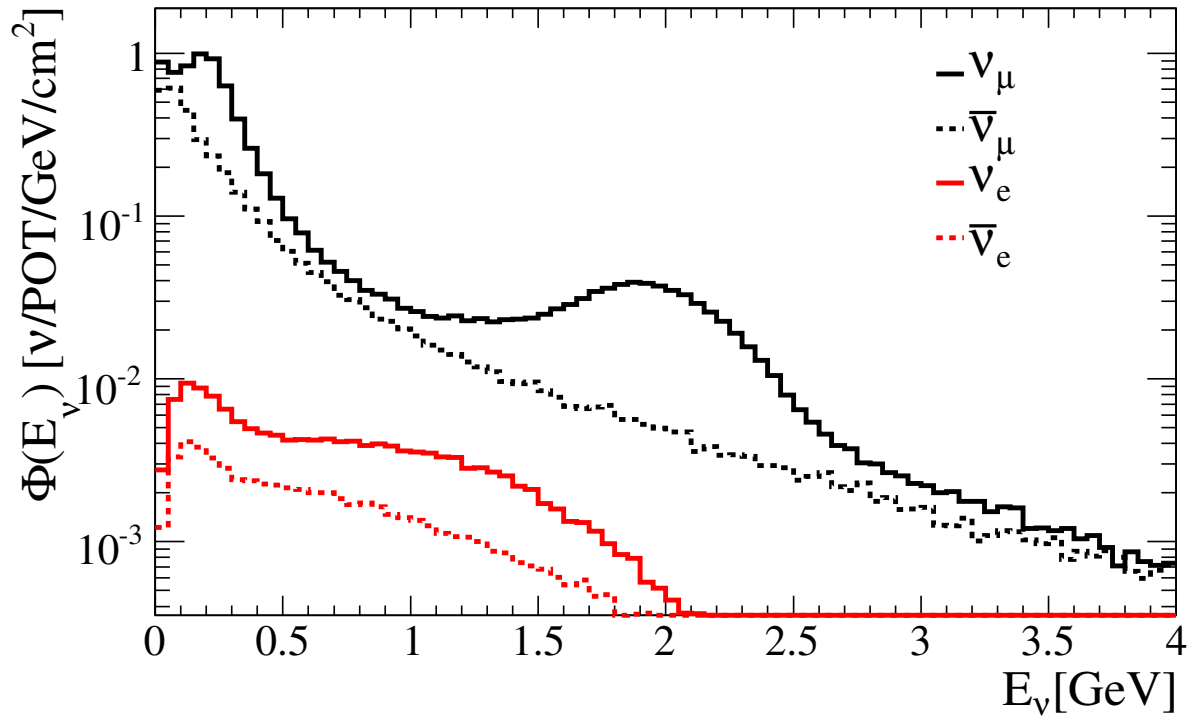
16

FIG. 13: *The NuMI beam.*

FIG. 14: *The estimated neutrino flux at the MiniBooNE detector from the NuMI beam.*
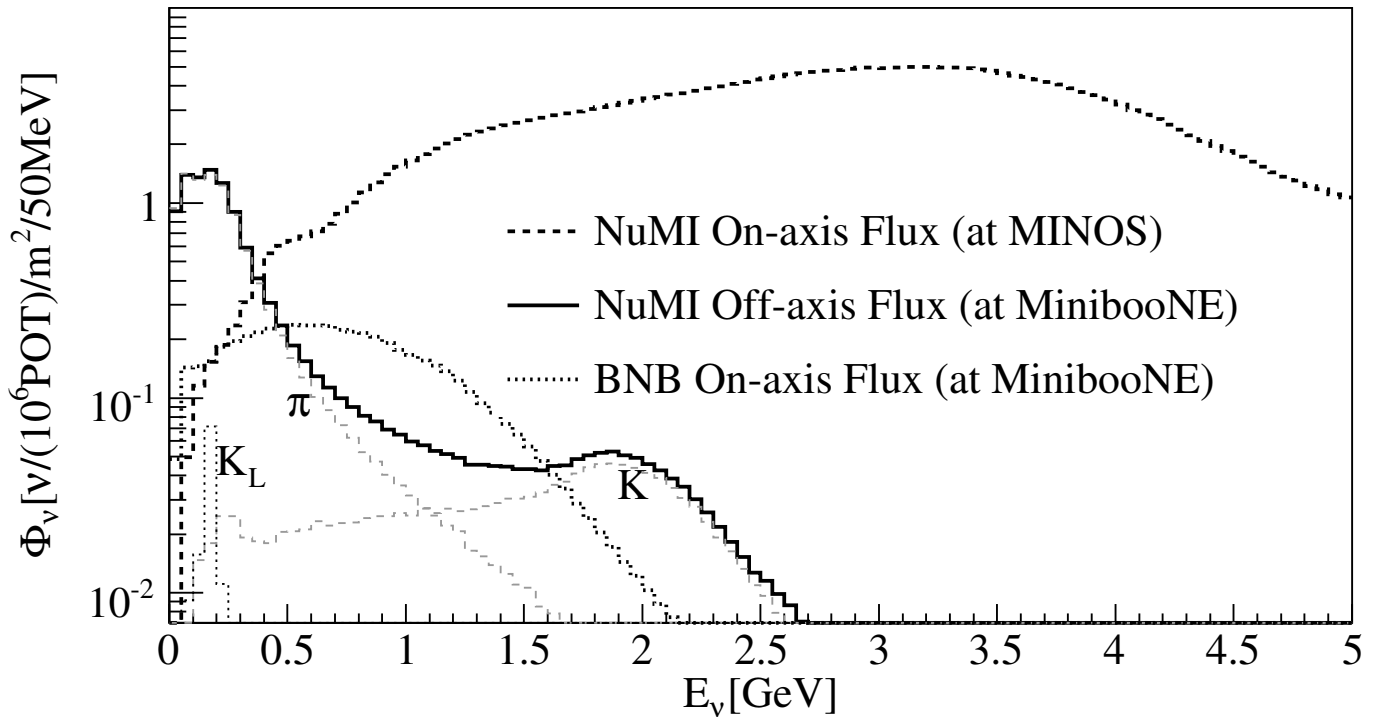
FIG. 15: *A comparison between the BNB and NuMI neutrino fluxes.*

reveal something profound about the nature of the ν_e sample.

PHYSICS GOALS WITH 1E21 POT IN ANTINEUTRINO MODE

MiniBooNE, so far, has collected $\sim 6.5 \times 10^{20}$ POT in neutrino mode and $\sim 3.4 \times 10^{20}$ POT in antineutrino mode. For the future, it is imperative to understand the MiniBooNE low-energy excess and to determine whether there is an unexpected difference between neutrino and antineutrino properties. The event excess in neutrino mode (and the apparent lack of an excess in antineutrino mode) is very interesting in its own right and important for future long-baseline experiments such as T2K. T2K will have a very similar neutrino energy distribution to MiniBooNE and will, therefore, be affected by the same low-energy excess. In addition, it is very important to test directly the LSND signal with a higher statistics antineutrino data sample. The ability of MiniBooNE to achieve these goals will require the collection of an additional 5E20 POT (1E21 POT total) in antineutrino mode. As discussed in Appendix D, this additional running time will take 1-3 years, depending on the BNB proton intensity.
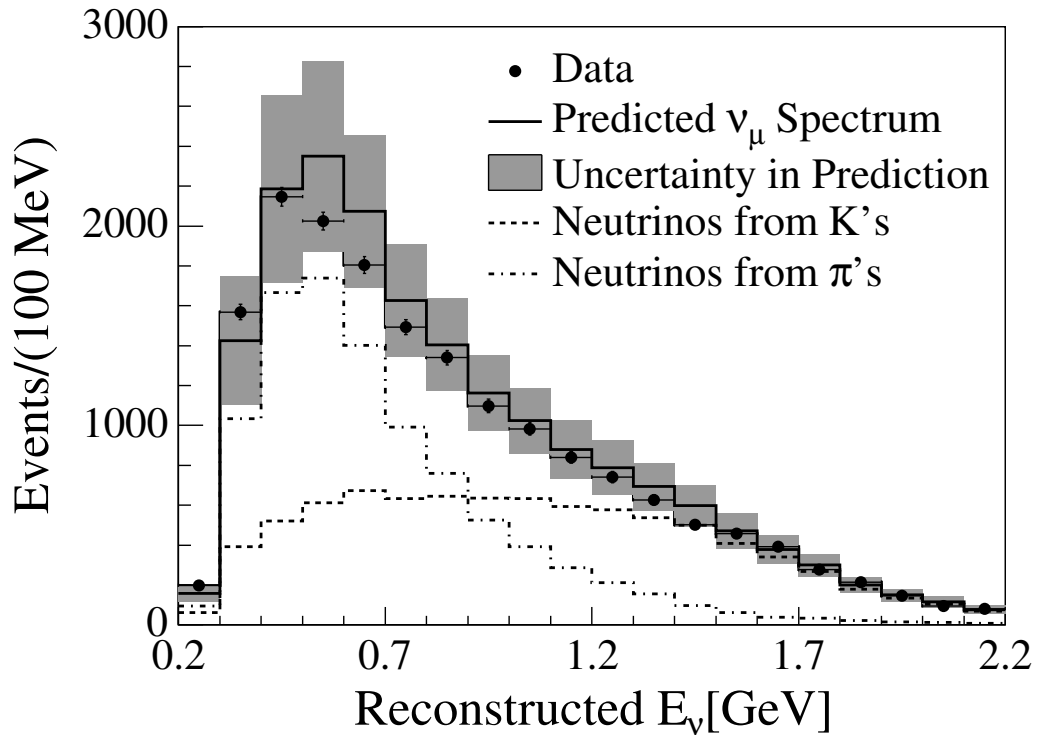
FIG. 16: *The comparison between data events (points with error bars) and the MC simulation (histogram) for NuMI-induced ν_μ CCQE candidate events.*

Testing the Low-Energy Excess with Antineutrinos

With 1E21 POT in antineutrino mode, MiniBooNE will be able to determine whether there is an anomalous difference between neutrino and antineutrino properties. Tables VI and VII show the expected excess of low-energy events in antineutrino mode under various hypotheses for 5E20 POT (approved) and 1E21 POT (requested), respectively. Also shown in the Tables is the probability (from a two-parameter fit to the data and assuming no excess in antineutrino mode) that each hypothesis explains the observed number of low-energy neutrino and antineutrino events, assuming only statistical errors, correlated systematic errors, and uncorrelated systematic errors. As can be seen in Table VII, the Neutrino Scaled hypothesis can be verified (and the other hypotheses rejected) with 1E21 POT if no excess is observed in antineutrino mode.
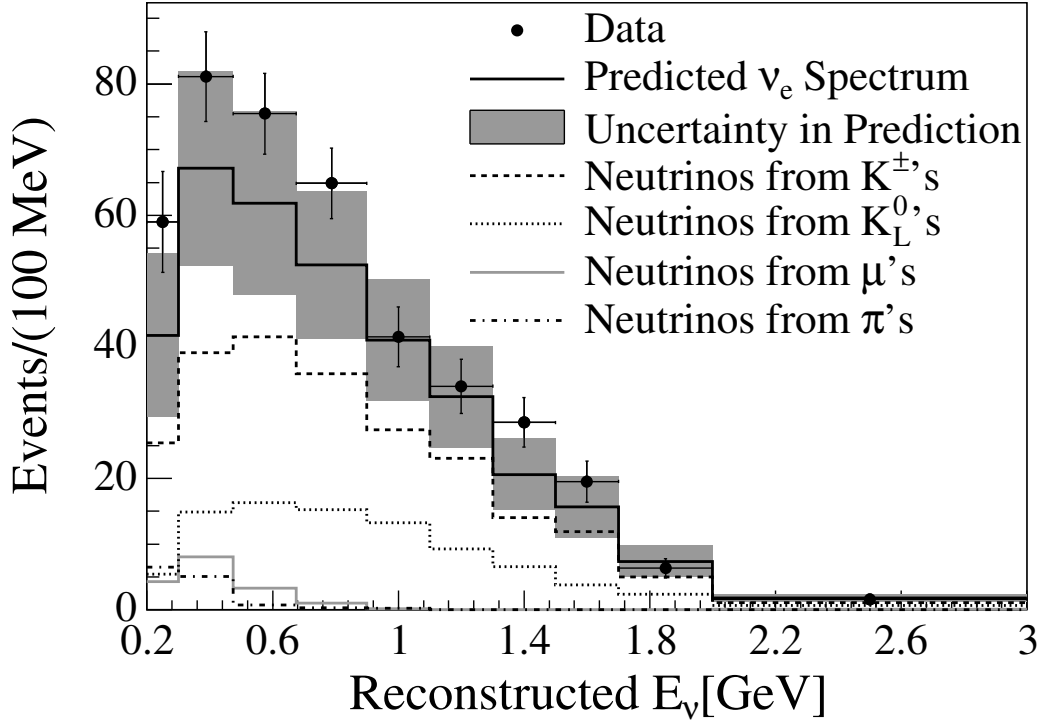
19

FIG. 17: *The comparison between data events (points with error bars) and the MC simulation (histogram) for NuMI-induced ν_e CCQE candidate events.*

TABLE VI: *The expected excess of low-energy events in antineutrino mode under various hypotheses for 5E20 POT. Also shown in the Table is the probability (from a two-parameter fit to the data and assuming no excess in antineutrino mode) that each hypothesis explains the observed number of low-energy neutrino and antineutrino events, assuming only statistical errors, correlated systematic errors, and uncorrelated systematic errors.*

Hypothesis	Expec. # of $\bar{\nu}$ Events	Stat. Err.	Cor. Syst. Err.	Uncor. Syst. Err.
Same σ	55.8	0.0%	0.0%	5.9%
π^0 Scaled	29.1	1.5%	3.9%	19.9%
POT Scaled	101.3	0.0%	0.0%	1.6%
BKGD Scaled	31.4	1.0%	2.6%	17.8%
CC Scaled	30.6	1.1%	3.0%	18.4%
Kaon Scaled	59.6	0.0%	0.0%	5.1%
Neutrino Scaled	10.1	32.5%	49.5%	57.9%

TABLE VII: *The expected excess of low-energy events in antineutrino mode under various hypotheses for 1E21 POT. Also shown in the Table is the probability (from a two-parameter fit to the data and assuming no excess in antineutrino mode) that each hypothesis explains the observed number of low-energy neutrino and antineutrino events, assuming only statistical errors, correlated systematic errors, and uncorrelated systematic errors.*

Hypothesis	Expec. # of $\bar{\nu}$ Events	Stat. Err.	Cor. Syst. Err.	Uncor. Syst. Err.
Same σ	111.6	0.0%	0.0%	4.7%
π^0 Scaled	58.2	0.1%	1.4%	17.1%
POT Scaled	202.5	0.0%	0.0%	1.3%
BKGD Scaled	62.7	0.1%	0.8%	15.0%
CC Scaled	61.2	0.1%	1.0%	15.6%
Kaon Scaled	119.1	0.0%	0.0%	4.0%
Neutrino Scaled	20.1	17.2%	44.1%	54.5%

A Direct Test of the LSND signal with Antineutrinos

With 1E21 POT in antineutrino mode, MiniBooNE will be able to make a direct test of the LSND signal. For the best-fit LSND point of $\Delta m^2 = 1.2$ eV^2 and $\sin^2 2\theta = 0.003$ [1], MiniBooNE should observe in the $475 < E_\nu^{QE} < 3000$ MeV energy range an excess of $\sim 40.0 \pm 15.2 \pm 20.9$ events, corresponding to a $\sim 1.5\sigma$ signal. The significance of such a signal may be improved by further reductions in the systematic uncertainties (e.g. by comparing antineutrino data to neutrino data). Fig. 18 shows the expected antineutrino oscillation sensitivity for a threshold energy of 475 MeV. The curves correspond to 3.4E20 POT, 5E20 POT, and 1E21 POT. With 1E21 POT, most of the LSND region is covered at 90% CL.

REQUEST

The MiniBooNE experiment observes an unexplained excess of electron-like events at low energies in neutrino mode, which may be due, for example, to either a neutral current radiative interaction [3] or to neutrino oscillations involving sterile neutrinos [4–8] which may
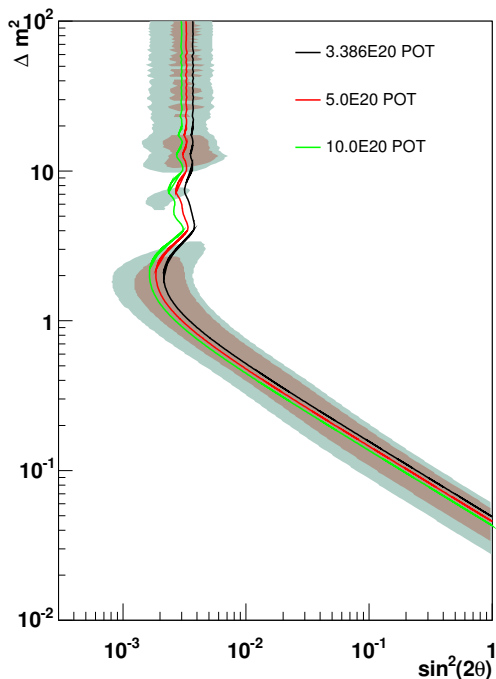
FIG. 18: *The expected antineutrino oscillation sensitivity for a threshold energy of 475 MeV. The curves correspond to 3.4E20 POT, 5E20 POT, and 1E21 POT.*

be related to the LSND signal. No excess of electron-like events, however, is observed so far at low energies in antineutrino mode. MiniBooNE, therefore, requests additional running in antineutrino mode for a total of 1E21 POT. With this additional data taking, which could be completed in one to three years (see Appendix D), the MiniBooNE collaboration will be able to determine conclusively whether there is an anomalous difference between neutrino and antineutrino properties. If, for example, there continues to be no low-energy excess in antineutrino mode with 1E21 POT, then the hypothesis that the excess scales as the neutrino flux (and not the antineutrino flux) would be confirmed and other hypotheses ruled out at > 98% CL.

In addition, the high energy antineutrino data will provide a direct test of the LSND signal and will increase the statistics of the NuMI data sample. With the present 3.4E20 POT in antineutrino mode, almost all of the LSND region is still allowed, as the current limit is worse than the sensitivity. However, with 1E21 POT in the case of no neutrino oscillations, most of the LSND allowed region should be ruled out. In the case of neutrino oscillations at the LSND best-fit point, a $\sim 1.5\sigma$ event excess would be expected.

22

ACKNOWLEGEMENTS

APPENDIX A: LIST OF MINIBOONE PUBLICATIONS

- A. A. Aguilar-Arevalo et al., Unexplained Excess of Electron-Like Events From a 1-GeV Neutrino Beam, [arXiv:0812.2243].

- P. Adamson et al., First Measurement of ν_μ and ν_e Events in an Off-Axis Horn-Focused Neutrino Beam, [arXiv:0809.2447].

- A. A. Aguilar-Arevalo et al., The Neutrino Flux prediction at MiniBooNE, [arXiv:0806.1449].

- A. A. Aguilar-Arevalo et al., The MiniBooNE Detector, Nucl. Instr. Meth. **A559**, 28 (2009).

- A. A. Aguilar-Arevalo et al., Compatibility of high-Δm^2 ν_e and $\bar{\nu}_e$ neutrino oscillation searches, Phys. Rev. **D78**, 012007 (2008).

- A. A. Aguilar-Arevalo et al., First Observation of Coherent Pi0 Production in Neutrino Nucleus Interactions with Neutrino Energy < 2 GeV, Phys. Lett. **664B**, 41 (2008).

- A. A. Aguilar-Arevalo et al., Measurement of Muon Neutrino Quasi-Elastic Scattering on Carbon, Phys. Rev. Lett. **100**, 032301 (2008).

- A. A. Aguilar-Arevalo et al., Search for Electron Neutrino Appearance at the $\Delta m^2 \sim 1$ eV^2 Scale, Phys. Rev. Lett. **98**, 231801 (2007).
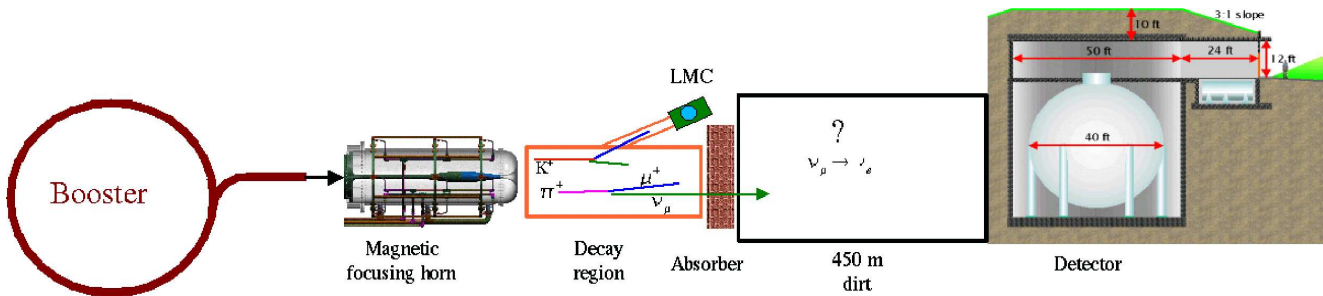
FIG. 19: *A schematic drawing of the MiniBooNE experiment.*

APPENDIX B: DESCRIPTION OF THE MINIBOONE EXPERIMENT

A schematic drawing of the MiniBooNE experiment at FNAL is shown in Fig. 19. The experiment is fed by 8-GeV kinetic energy protons from the Booster that interact in a 71-cm long Be target located at the upstream end of a magnetic focusing horn. The horn pulses with a current of 174 kA and, depending on the polarity, either focuses π^+ and K^+ and defocuses π^- and K^- to form a neutrino beam or focuses π^- and K^- and defocuses π^+ and K^+ to form a less pure antineutrino beam. The produced pions and kaons then decay in a 50-m long pipe, and the resulting neutrinos and antineutrinos [23] can then interact in the MiniBooNE detector, which is located 541 m downstream of the Be target. For the MiniBooNE results presented here, a total of 6.5×10^{20} POT were collected in neutrino mode and 3.4×10^{20} POT were collected in antineutrino mode.

The MiniBooNE detector [24] consists of a 12.2-m diameter spherical tank filled with approximately 800 tons of mineral oil (CH_2). A schematic drawing of the MiniBooNE detector is shown in Fig. 20. There are a total of 1280 8-inch detector phototubes (covering 10% of the surface area) and 240 veto phototubes. The fiducial volume is a 5-m radius that corresponds to approximately 450 tons. Only $\sim 2\%$ of the phototube channels failed over the course of the run.
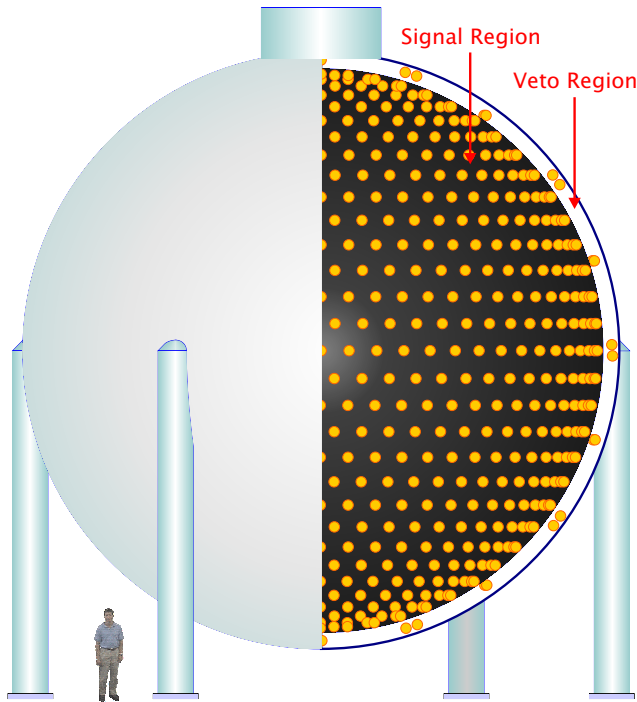
MiniBooNE Detector

FIG. 20: *A schematic drawing of the MiniBooNE detector.*

APPENDIX C: MINIBOONE CROSS SECTION RESULTS

MiniBooNE has published two cross section results. First, MiniBooNE has made a precision measurement of ν_μ charged-current quasi-elastic (CCQE) scattering events [25]. Fig. 21 shows the ν_μ CCQE Q^2 distribution for data (points with error bars) compared to a MC simulation (histograms). A strong disagreement between the data and the original simulation (dashed histogram) was first observed. However, by increasing the axial mass, M_A, to 1.23 ± 0.20 GeV and by introducing a new variable, $\kappa = 1.019 \pm 0.011$, where κ is the increase in the incident proton threshold, the agreement between data and the simulation (solid histogram) is greatly improved. It is impressive that such good agreement is obtained by adjusting these two variables.

MiniBooNE has also collected the world's largest sample of neutral-current π^0 events [26], as shown in Fig. 22. By fitting the $\gamma\gamma$ mass and $E_\pi(1 - \cos\theta_\pi)$ distributions, the fraction of π^0 produced coherently is determined to be $19.5 \pm 1.1 \pm 2.5\%$. Excellent agreement is obtained between data and MC simulation.
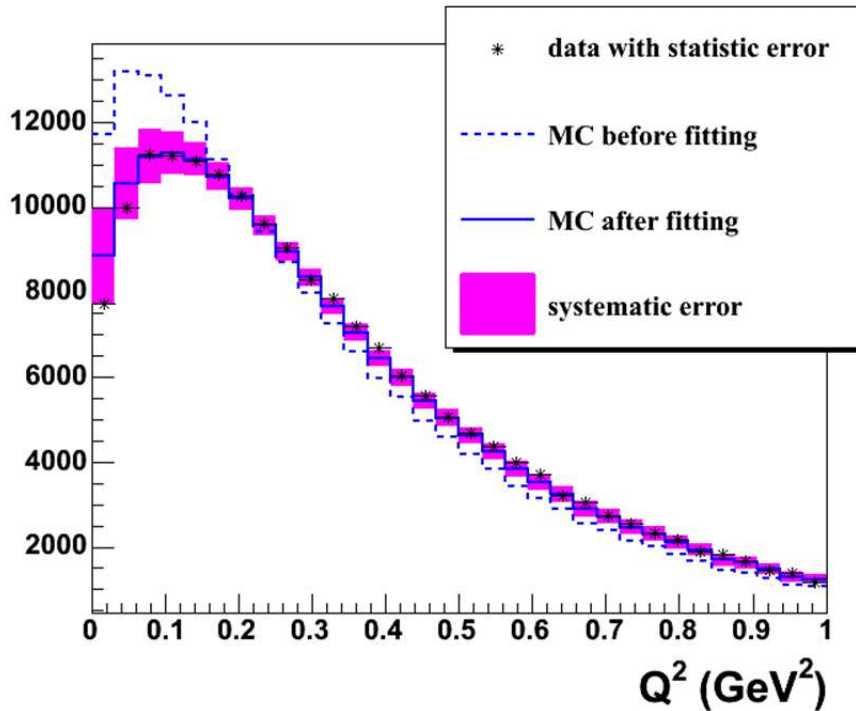
FIG. 21: *The ν_μ CCQE Q^2 distribution for data (points with error bars) compared to the MC simulation (histograms) for the neutrino data sample.*

APPENDIX D: PROTON PROJECTIONS AND RUN FEASIBILITY

The achievement of the physics goals outlined above depends critically on the experiment's ability to complete the run, i.e., how long will it take to collect the data given current POT projections, and assuming various scenarious for increased POT? Are there sufficient personnel to staff shifts and do the analysis? Is the apparatus sufficiently robust? and are there enough spare parts?

By the summer shutdown of June 2009, we expect to reach our initial goal of 5E20 POT. Figure 23 shows the current POT levels and projections to the end of run at the June 2009 shutdown. As of the writing of this report, we have 4.54E20 POT. This is far better than the expected Booster output projections (green line). The better than expected performance is due to about two and a half months of NuMI down time when our beam rates went up by about a factor of three. With about five months left in the current run, we should reach our goal of 5E20 POT in antineutrino mode if our uptime remains at current levels.

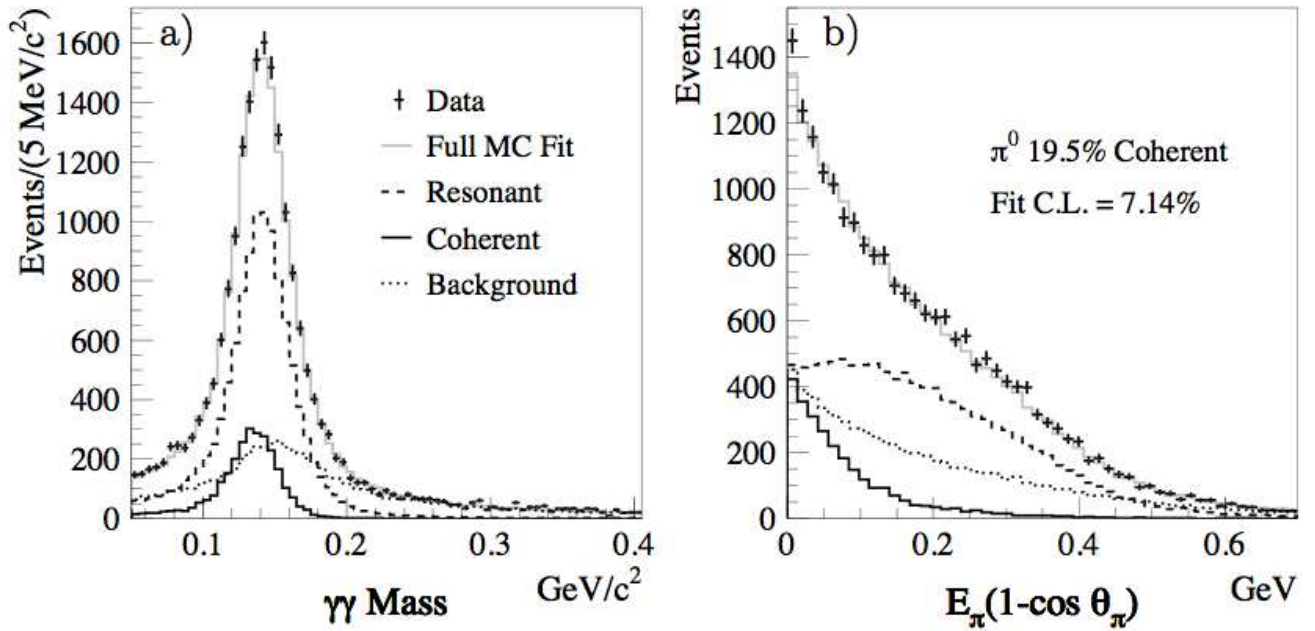During peiods when NuMI is running and taking full beam, we average about 2.2E16

27

FIG. 22: *The neutral-current π^0 $\gamma\gamma$ mass and $E_\pi(1-\cos\theta_\pi)$ distributions for data (points with error bars) compared to the MC simulation (histograms) for the neutrino data sample.*

POT/hr and 85% uptime, which translates into 3.2E18 POT/week. Assuming a 43 week run period (9 weeks less for summer shutdowns), then this give us 1.5E20 POT per year at current rates. Thus, to collect an extra 5E20 POT will take about three years. Table shows the protons per hour, per week, and time required for an extra 5E20 POT (total of 10E20 POT) in antineutrino mode assuming different beam delivery rate scenarios. Increased beam to BNB comes at the expense of NuMI (deliberately throttled back) or increases to Booster output. It is apparent that there is a large impact in the run time (1-3 years) necessary to collect the requested POT depending on proton management decisions or improvements to the Booster output.

The success of the run requires the personnel to staff shifts, and the reliability of the hardware and availability of spare parts for a further two years of operations. At present, we are still working the exact number of personnel available for shifts, but is expected to be about 25 to 40 FTE's. This is barely enough to staff shifts over a long period of time. However, during the 2008-2009 run, MiniBooNE developed the capability for staffing shifts at remote locations. So far, we have eight institution with remote control room capability. This facilitates the ability of collaborators to meet their shift requirements with minimal
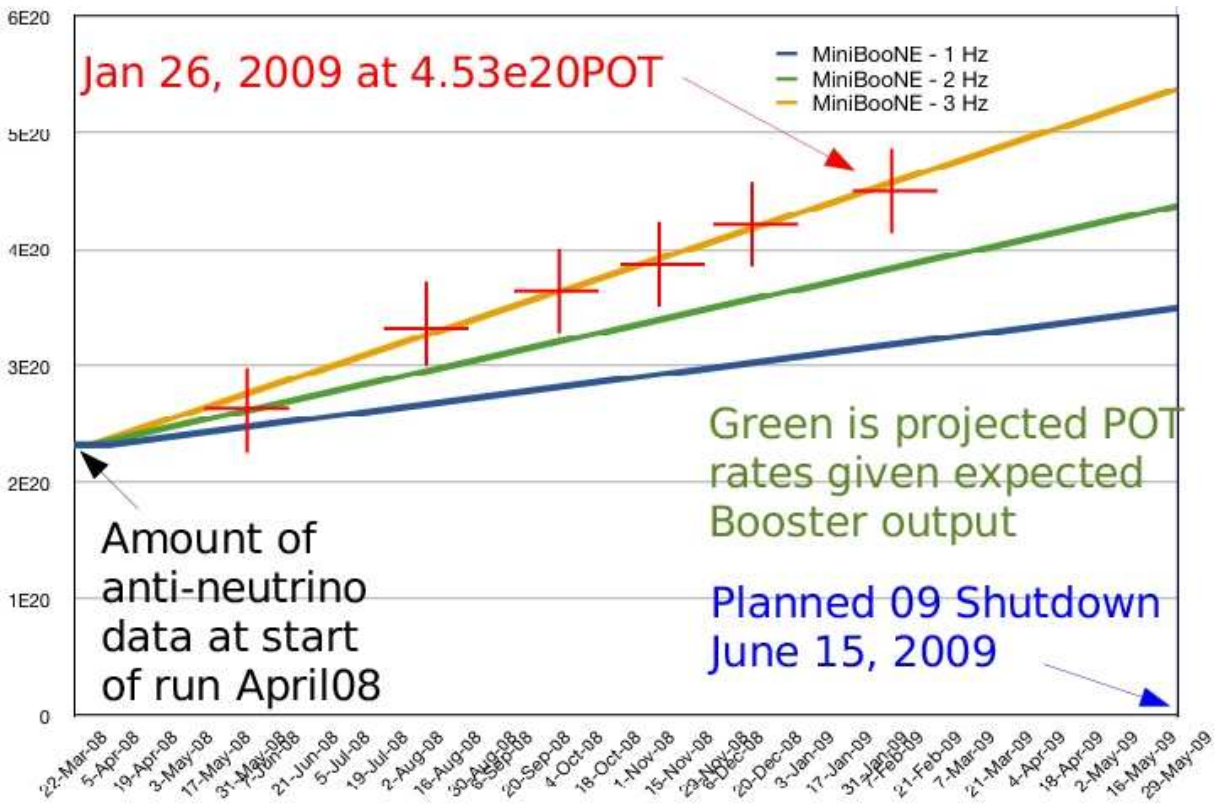
FIG. 23: *POT projections for the current antineutrino run.*

travel and disruption to their scheule. This has been working extremely well for the last six months and has given MiniBooNE new life in its ability to staff shifts and keep the experiment running. This will be instrumental for the success of any future running.

The beamline, horn system, and detector have been operating well for the duration of the experiment since 2002. One horn replacement has been needed, and a repair of the 25 m absorber in 2006, but no other major downtime have been incurred. A third horn and target are ready, as are spare accelerator parts, and spare detector electronics sufficient to run the experiment for up to three more years. Also available is a fourth horn inner conductor (the part with the longest lead time). One possible trouble spot is the detector HVAC, which has been problematic over the years. If we are given the go ahead for further running, then thought should be given to replacing the current HVAC, which would improve detector operations. An inspection of the 25 m absorber during the 2007 shutdown shows it to be working well with no corrosion present on the new hanging fixtures. Another inspection will be performed during the 2009 summer shutdown.

29

Rate increase	proton/hr	proton/week	protons/year	Years to 5E20 POT
Nominal	2.2E16	3.2E18	1.5E20	3.3
50% increase	3.3E16	5.3E18	2.3E20	2.2
100% increase	4.4E16	6.4E18	3.0E20	1.7
Maximum increase	7.5E16	10.7E18	4.6E20	1.1

TABLE VIII: *Number of years to collect an extra 5E20 POT (total of 10E20 POT) in antineutrino mode assuming various run conditions. "Nominal" is for the current rate of protons delivered to BNB. The increase in protons delivered comes at the expense of protons delivered to NuMI, or increased output of the Booster, with the "Maximum" row corresponding to the maximum that the Booster can currently deliver on a long term basis to the neutrino program.*

With everything in place from the ν_e and $\bar{\nu}_e$ appearance analysis that have been presented, these same tools will be repeated for the extra data collected. Also, work is currently ongoing to perform a combined ν_e and $\bar{\nu}_e$ appearance analysis in which many common systematic errors will cancel and tests the difference between ν_e and $\bar{\nu}_e$ expectations. Results on this should be avaialble in mid to late 2009, including the extra data from the current run. There will likely be some fresh optimizing of cuts and tuning of simulations, but nothing compared to the level of work required to produce the ν_e appearance result. Consequently, $\bar{\nu}_e$ appearance and combined analysis results are expected to be available shortly after the extra 5E20 POT is accumulated.

[1] C. Athanassopoulos *et al.*, Phys. Rev. Lett. 75, 2650 (1995); 77, 3082 (1996); 81, 1774 (1998); A. Aguilar *et al.*, Phys. Rev. D 64, 112007 (2001).

[2] A. Aguilar-Arevalo *et al.*, Phys. Rev. Lett. 98, 231801 (2007); A. Aguilar-Arevalo *et al.*, submitted to Phys. Rev. Lett., [arXiv:0812.2243].

[3] Jeffrey A. Harvey, Christopher T. Hill, Richard J. Hill, [arXiv:0708.1281]; [arXiv:0712.1230].

[4] Michel Sorel, Janet Conrad, and Michael Shaevitz, Phys. Rev. D 70, 073004 (2004); C. Karagiorgi *et al.*, Phys. Rev. D 75, 013011 (2007); Alessandro Melchiorri *et al.*, [arXiv:0810.5133].

[5] Heinrich Paes, Sandip Pakvasa, Thomas J. Weiler, Phys. Rev. D 72, 095017 (2005); [arXiv:hep-ph/0504096].

[6] T. Goldman, G. J. Stephenson Jr., and B. H. J. McKellar, Phys. Rev. D 75, 091301 (2007).

[7] Michele Maltoni and Thomas Schwetz, Phys. Rev. D 76, 093005 (2007); [arXiv:0705.0197].

[8] Ann E. Nelson and Jonathan Walsh, [arXiv:0711.1363].

[9] B. T. Cleveland *et al.*, Astrophys. J. 496, 505 (1998).

[10] J. N. Abdurashitov *et al.*, Phys. Rev. C 60, 055801 (1999).

[11] W. Hampel *et al.*, Phys. Lett. B 447, 127 (1999).

[12] S. Fukuda *et al.*, Phys. Lett. B 539, 179 (2002).

[13] Q. R. Ahmad *et al.*, Phys. Rev. Lett. 87, 071301 (2001); Q. R. Ahmad *et al.*, Phys. Rev. Lett. 89, 011301 (2002); S. N. Ahmed *et al.*, Phys. Rev. Lett. 92, 181301 (2004).

[14] K. Eguchi *et al.*, Phys. Rev. Lett. 90, 021802 (2003); T. Araki *et al.*, Phys. Rev. Lett. 94, 081801 (2005).

[15] K. S. Hirata *et al.*, Phys. Lett. B 280, 146 (1992); Y. Fukuda *et al.*, Phys. Lett. B 335, 237 (1994).

[16] Y. Fukuda *et al.*, Phys. Rev. Lett. 81, 1562 (1998).

[17] W. W. M. Allison *et al.*, Phys. Lett. B 449, 137 (1999).

[18] M. Ambrosio *et al.*, Phys. Lett. B 517, 59 (2001).

[19] M. H. Ahn *et al.*, Phys. Rev. Lett. 90, 041801 (2003).

[20] D. G. Michael *et al.*, Phys. Rev. Lett. 97, 191801 (2006); P. Adamson *et al.*, Phys. Rev. Lett. 101, 131802 (2008).

[21] T. Katori, A. Kostelecky and R. Tayloe, Phys. Rev. D 74, 105009 (2006).

[22] P. Adamson *et al.*, [arXiv:0809.2447].

[23] A. Aguilar-Arevalo *et al.*, [arXiv:0806.1449].

[24] A. Aguilar-Arevalo *et al.*, Nucl. Instr. Meth. **A559**, 28 (2009).

[25] A. Aguilar-Arevalo *et al.*, Phys. Rev. Lett. 100, 032301 (2008).

[26] A. Aguilar-Arevalo *et al.*, Phys. Lett. 664B, 41 (2008).